Numerical Solution Verification for a Generic, Point-absorber Wave Device

G. Parisella, A. J. C. King

School of Civil and Mechanical Engineering
and Fluid Dynamics Research Group
Curtin University, Western Australia 6102, Australia

Abstract

The fluid-flow problem relative to wave-energy conversion is solved using a variety of methods, often including potential theory, computational fluid dynamics (CFD) and/or wave-tank experiments. Amongst them, CFD is highly valued for its accuracy and its capability to potentially replace the experiments at a fraction of the costs.

Being a common engineering tool in many industries, its continuous evolution and recent availability of open-source codes contribute to the popularity of the CFD method also in the field of marine hydrodynamics. Though investigation of accuracy for both tool and numerical solution involves a good amount of time and resources (in addition to the already high base-costs of the method), and often the verification activity is given low priority during the wave energy converter (WEC) development phase. While the current literature provides a good amount of CFD validation and verification (V&V) examples for many fluid-flow problems, only a small number of cases are found for marine hydrodynamics that closely relate to wave energy devices. Furthermore, those publications are mostly focused on validation, that is the comparison of the numerical solution with experimental data.

The use of CFD simulations to explore potential design solutions is well accepted, therefore the uncertainty of numerical results should matter. Here, the motion of a generic heave point-absorber is simulated under the excitation of a regular sea-state. The procedure described in the "ASME V&V 20-2009" Standard is applied to the calculated solutions, for which spatial and temporal discretisation uncertainties are estimated, along with the influence of parameters relevant to the problem, e.g. the numerical wave tank setup. The results of the solution verification exercise are presented to allow increased certainty in the results gained using CFD for wave energy studies.

While a specific WEC is studied in this work, the case stands as a reference for other researchers. Also the method implementation is extendable to other devices.

Background

Calculations obtained from computer models should give a good accuracy and implement the conceptual model without errors. Although this outcome is the aim, the extent to which it is met is often not quantified.

Terminology (and knowledge) in regard of Verification and Validation (V&V) activities has been clarified with the contribution of several authors and organisations across the last several decades, see for example [1, 18, 14, 15, 19] with more found in the literature. *Verification* relates to the implementation of the mathematical model, assessing the accuracy of a computed solution in comparison to a known accurate one. *Validation* relates to the suitability of a mathematical model to the physical events it tries to emulate, assessing the computed solution in comparison to experimental data.
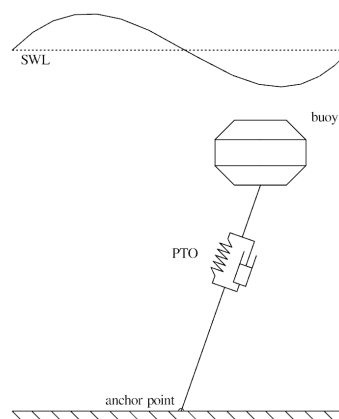
Figure 1: WEC device schematic diagram

V&V are the primary means to assess accuracy and reliability in computational simulations, though there are many examples in the literature where validation was claimed upon graphical agreement of results, in fact providing a qualitative assessment only, [15]. Perhaps for a variety of reasons, quantitative V&V activities are not commonly reported, [20], even more so amongst wave energy applications.

The five major sources of errors in CFD are, [15]: insufficient spatial discretisation convergence, insufficient temporal discretisation convergence, insufficient convergence of an iterative procedure, computer round-off, and computer programming errors. The first 4 items are investigated through *solution verification*, while the programming errors are investigated through *code verification*. This work is mainly focused on the solution verification. The OpenFOAM code verification (i.e. software testing) was not found in literature, and the code functionality can only be appreciated through its many applications found in the literature. Since the late 80's, the Journal of Fluids Engineering has introduced a "Policy on the Control of Numerical Accuracy" requiring papers to satisfy a list of ten criteria in order to be considered for acceptance, [10]. Reviews of procedures/methods are found in [6, 17]. Several publications provide examples where V&V was applied, see [7, 8, 13] and more are found in the literature.

Approach

OpenFOAM (version v1706) solvers *interFoam* and its variant *overInterDyMFoam* were used to produce the numerical results in this work. They are Finite Volume method solvers for two incompressible fluids, with Volume of Fluid (VOF) interface capturing approach. The Reynolds averaged Navier–Stokes equations were solved with the *PIMPLE* algorithm, combining PISO and SIMPLE iterative procedures, [16]. No code customisation was required, and the cases were run with the original Open-FOAM source code. The wave propagation was possible us-

ing the dedicated (velocity) boundary conditions implemented in OpenFOAM, and described in [11]. The code allowed for active absorption of (normal) waves at the boundaries, reducing the reflection to levels equal or below 10% of the wave amplitude.

Boundary conditions at solid walls generally considered zero-gradient (Neumann) condition for the pressure, and no-slip (Dirichlet) condition for the velocity. Inlet/outlet patches considered a pressure gradient corrected for mass conservation, and velocities imposed by the wave field. The atmosphere (top) boundary considered zero (atmospheric) pressure and zero velocity gradient for an outward flow, while it used corrected pressure with calculated normal velocity for an inward flow.

The numerical schemes generally considered a blended Crank–Nicolson/Euler scheme for the time derivative, with 0.5 blending factor resulting in a theoretical order of 1.5. A second-order vanLeer scheme was used for the convection of the volume fraction (α), while a linear (central) scheme was used for the velocity and the diffusion terms. Effects of different numerical schemes were not assessed. Also, no turbulence model was applied for the presented cases.

The solution verification was performed according to the ASME procedure [2], for which the main expressions are reported next. A set of three grids N_1, N_2, N_3 (fine to coarse) with representative mesh size h_1, h_2, h_3 are required. A refinement factor is defined as $r_{21} = h_2/h_1$. Denoting the i-th grid solution as ϕ_i, the changes are defined as $\varepsilon_{32} = \phi_3 - \phi_2$ and $\varepsilon_{21} = \phi_2 - \phi_1$. The observed method order is then given as $p = \frac{1}{ln(r_{21})}|ln|\varepsilon_{21}/\varepsilon_{21}| + q(p)|$ with $q(p)$ depending on the grid refinements. The extrapolated solution is defined as $\phi_{ext}^{21} = (r_{21}^p \phi_1 - \phi_2)/(r_{21}^p - 1)$. The approximate relative error is $e_a^{21} = |\frac{\phi_1 - \phi_2}{\phi_1}|$ from which the fine-grid convergence index is calculated as $GCI_{fine}^{21} = \frac{1.25 e_a^{21}}{r_{21}^p - 1}$ corresponding to the numerical uncertainty u_{num} without assumptions on the error distribution.

Numerical Wave Tank

First, a two-dimensional numerical wave tank (NWT) was simulated. This case is relevant to assess the effects of different input/settings to the wave propagation that is later used to estimate wave-power absorption. Relevant references are [11] and [9]. Numerical wave tank studies can be found in the literature, for example [4] indicates mean diffusive errors within 10% of the wave height after 15 periods.

This case considered a rectangular computational domain of $312m \times 22m$, with 20m water depth. Tank length was chosen to allow for at least two wave lengths (deep water). A single cell in transverse (y) direction made the model two-dimensional in OpenFOAM. Generally, the grid (regular) was discretised with 200 cells per wave length (deep-water) and 5 cells per wave height, except for spatial-grid variations. The wave condition was regular waves of 0.5m wave height and 10s peak period, with a wave length of 121.2m. This case is considered intermediate depth and a Stokes 2nd order theory is applicable. The wave length is slightly shorter than a deep water case (156m).

Solution verification according to the ASME procedure [2] was applied to the finer 568 x 321 grid. Fast Fourier Transform was applied to the time signals, and presented solutions ϕ_i include the main (1st) amplitude component only. The point-variables of interest were: phase fraction (α), velocity ($\mathbf{u}$), and pressure (p). A probe (line) was located at mid-length ($x = 156m$) and a depth of $z = -2m$ was used to study velocity and pressure values. Simulated time accounted for 50 wave periods, with calculations generally using a time-step $dt = 0.001s$. Time discreti-
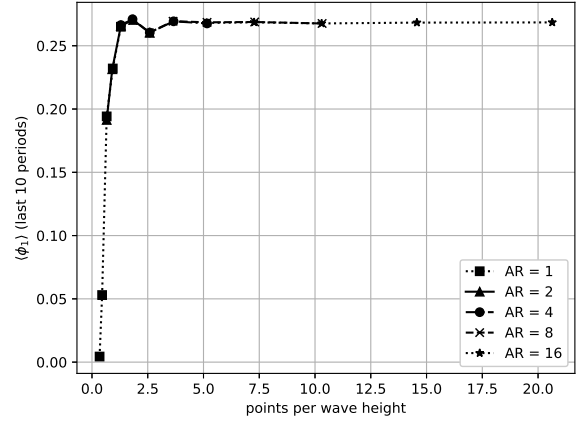
Figure 2: NWT solution η at different cell aspect ratios
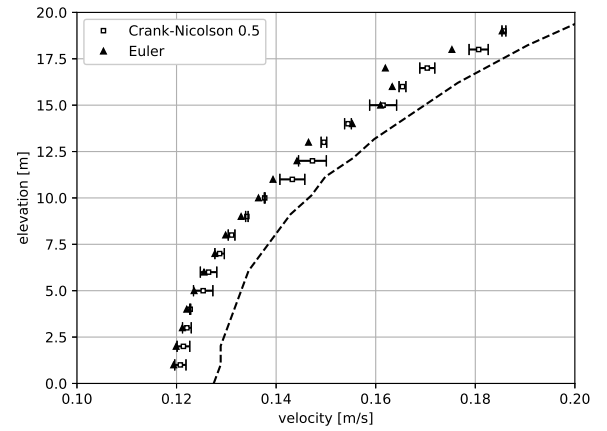
Figure 3: NWT finer-grid solution of velocity u with error bars, and theoretical profile

sation was observed using different time-step sizes of 0.0005, 0.001, 0.002s. A very small relative error was found for the wave elevation η between the dt. A different influence was observed in terms of velocity amplitudes, for which both mean (zero-th) and first FFT component amplitudes presented oscillations at larger time-step size, see figure 4.

In figure 3, the relative error is found in the range 6-10% from the theoretical data. Note that the discretisation error bars in figure 3 express the averaged computed order $p_{ave} = 1.63$.

	η	u	w	p
N_1, N_2, N_3		91027, 45280, 22600		
r		2		
ϕ_1	0.269	0.172	0.146	2436
ϕ_2	0.269	0.172	0.146	2450
ϕ_3	0.269	0.174	0.147	2429
p	1.74	2.00*	2.00*	0.57
e_a^{21}	0.10%	0.05%	0.47%	0.57%
GCI_{fine}^{21}	0.05%	0.10%	0.02%	1.47%

Table 1: NWT spatial discretisation uncertainty

* Observed method order limited to theoretical value.

Heave Decay Test

This case considered heave motion decay for a floating cylinder. It is relevant to explore the moving mesh features (overset grid), and further increase confidence in the CFD model leading to
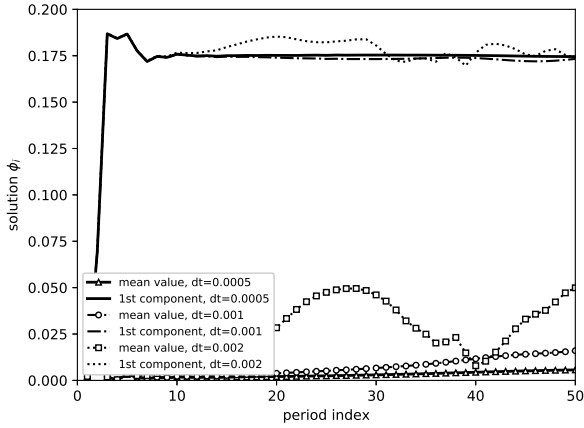
Figure 4: NWT per-wave solution of velocity u for timestep variation

Figure 5: Floating cylinder damping coefficient in heave, and relative GCI band

the WEC device simulation. Reference case and experimental damping coefficients are taken from [21]. The theory in regard of the heave motion decay analysis is well described in [12].

The three-dimensional rectangular domain ($16m \times 8m \times 4m$) consisted of a mixed grid with 96% hexahedral cells. A floating cylinder (diameter D=0.457m) was placed halfway the tank length. And a longitudinal symmetry plane divided the domain in two halves reducing the computational costs. The grid size was approx 100cells per wave length and 5cells per wave height near the free surface, with coarser cells' height towards the bottom. The cells were further split near the cylinder surface.

The cylinder was constrained to move in heave only. It was initially displaced of a set amount, and released at the simulation start. The oscillation amplitude dissipated with time until it reached the equilibrium. This simulation differed from the original experiments where the cylinder was forced to oscillate. A discrepancy may be found in regard of the KC number ($KC = 2\pi x/D$), computed from the FFT amplitude of the first oscillation period, though it was deemed sufficient to verify the overset grid implementation for the purposes of this exercise.

The main parameter of interest was the position of the cylinder (centre of mass) in time. From its history, a solution to the equation of motion $\ddot{z} + 2\kappa\omega_0\dot{z} + \omega_0^2 z = 0$ can be obtained and the damping coefficient computed, [12]. The verification considered three systematically refined grids applied at two different initial displacements. The grid refinement factor was $r = 2$, considering the cells' volume.

Considering the damping coefficient, the minimum computed order of the method was 1.26 corresponding to a maximum GCI of 4.7%. In terms of oscillation frequency, the resulting range was 0.425-0.439Hz accounting for a maximum relative error of 6.6% in comparison to 0.41Hz from [21].

WEC Device

A wave-energy device model (see figure 1) was built and simulated considering observations from previous cases. It constitutes the core case of this work.

The device geometry and work principle are adopted from the case *Bref-SHB* included in [3]. It originates from an earlier version of the CETO technology from Carnegie Clean Energy [5]. The WEC consisted of a submerged buoy (diameter D=7m) tethered to the bottom floor. Its motion, mainly surge and heave, activates a power take-off unit from which energy is collected and/or stored. The linear PTO unit provided the restoring
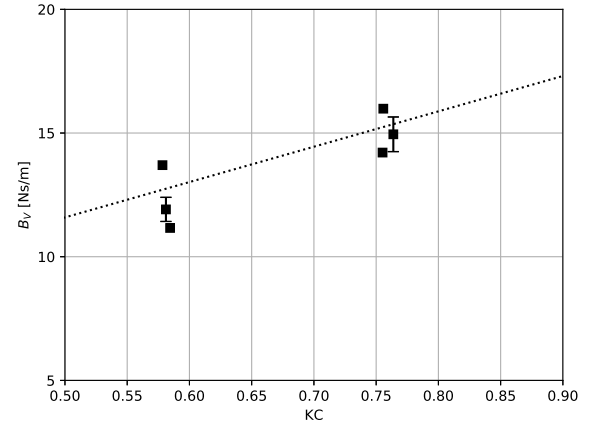
spring and damping with set values of $K_{PTO} = 120$kN/m and $B_{PTO} = 60$kN/ms, respectively [3].

The computational (3D) domain size was $180m \times 45m \times 24m$, with a water depth of 20m. A longitudinal plane of symmetry was adopted, therefore constraining the buoy motion in-plane only. Rotations were also constrained to improve the simulation stability. The mesh was produced with the OpenFOAM built-in module *snappyHexMesh*, and it contained mostly hexahedral cells (99%). The domain was sized to accomodate two wave lengths ($\lambda = 88.8m$), and the finer grid discretised with 200 cells per wave. Though, substantial refinement was applied to cells height in the (calm) free-surface region and around the buoy surface.

A mild regular wave condition was imposed, with a wave height of 0.5m and a period of 8s.

The main observed quantities were the buoy position (**x**) and its surface load (**F**). The method used to produce the grid was difficult to tune in terms of cell size consistency, although it aimed at systematic refinements. Some discrepancies were found for the cells' volume in relation to the goal refinement, therefore the median cell volume was used in this case. Simulation instabilities were encountered for some of the grids, hence it was necessary to adopt the *Euler* time scheme corresponding to a formal order $p = 1$.

Although five grids were simulated with a number of cells in the range 1.7–0.4M, the grids (2,3,4) presented better convergence for the variables of interest **x** and **F**, therefore it was used for computing the numerical uncertainty, see table 2 and figure 6. Point-variables wave elevation η, flow velocity u and pressure p presented monotonic convergence for the grids (1,2,3).

	$mag(\mathbf{x})$	$mag(\mathbf{F})$	η	u	p
N_1,N_2,N_3	1.24M, 0.87M, 0.61M		1.67M, 1.24M, 0.87M		
r		1.40		1.40	
ϕ_1	0.323	8208	0.225	0.206	1950
ϕ_2	0.309	8383	0.235	0.205	2054
ϕ_3	0.254	6535	0.292	0.299	3726
p	2.00*	2.00*	2.00*	2.00*	2.00*
e_a^{21}	4.52%	2.14%	4.49%	0.61%	5.34%
GCI_{fine}^{21}	5.89%	2.78%	5.85%	0.80%	6.95%

Table 2: WEC device spatial discretisation uncertainty

Simulated time accounted for 50 wave periods with a timestep $dt = 0.01s$. Time discretisation was observed using different
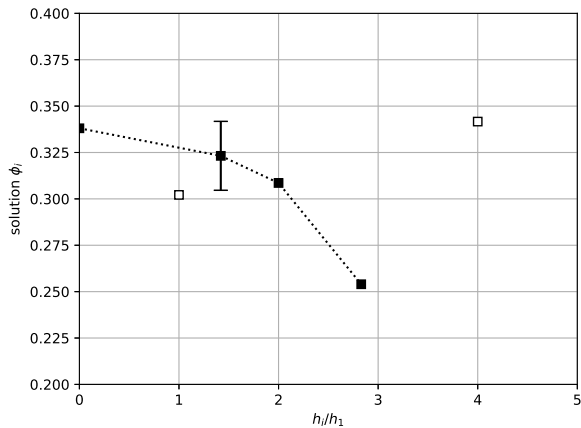
Figure 6: WEC's motion amplitude (empty markers for discarded grids)

step sizes of 0.001, 0.002, 0.005 and 0.01s. Convergence for temporal refinements was monotonic for position and oscillatory for pressure load magnitude with a maximum observed GCI less than 1% for the smaller timestep, which resulted in a coarse-timestep uncertainty of 5.6% in this case.

Conclusions

A verification exercise following the ASME Standard was performed for a wave energy converter. The numerical model was built in steps, facilitating the path leading to the transient simulation using the built-in OpenFOAM overset (dynamic) mesh capability. Initially, a 2D numerical wave tank and a 3D heave decay test for a floating cylinder were simulated, both resulting in numerical uncertainties within 10% for a theoretical method order of 2. Finally, the wave device was simulated. Difficulties in solution convergence were observed at different levels and even for its finer grids. Spatial and temporal uncertainties for the integral variables, position ($\mathbf{x}$) and force ($\mathbf{F}$), were estimated to be up to 6%. Further work to extend this study of numerical uncertainties is planned, including the application of different verification procedures to overcome the issues related to grids with problematic convergence.

Acknowledgements

References

[1] AIAA, S. C. et al., Guide for the Verification and Validation of Computational Fluid Dynamics Simulations, 1998.

[2] ASME, V. C. et al., Standard for verification and validation in computational fluid dynamics and heat transfer, 2009.

[3] Babarit, A., Hals, J., Kurniawan, A., Muliawan, M., Moan, T. and Krokstad, J., The NumWEC project: Numerical estimation of energy delivery from a selection of wave energy converters, *Ecole Centrale de Nantes, Tech. Rep.*

[4] Bruinsma, N., *Validation and application of a fully nonlinear numerical wave tank*, Ph.D. thesis, TUDelft, Delft University of Technology, Netherlands, 2016.

[5] Carnegie Clean Energy, Wave - Carnegie Clean Energy, 2018.

[6] Eça, L., An Evaluation of Verification Procedures for CFD Applications, in *24th Symposium on Naval Hydrodynamics, Fukuoka, Japan*, 2002, 568–587, 568–587.

[7] Eça, L., Hoekstra, M. and Roache, P., Verification of calculations: an overview of the Lisbon workshop, in *23rd AIAA Applied Aerodynamics Conference*, 2005, 4728, 4728.

[8] Eça, L., Hoekstra, M., Roache, P. and Coleman, H., Code verification, solution verification and validation: an overview of the 3rd Lisbon workshop, in *19th AIAA Computational Fluid Dynamics*, American Institute of Aeronautics and Astronautics, 2009, 3647.

[9] Fenton, J., Nonlinear wave theories, *The Sea-Ocean Engineering Science*, **9**, 1990, 3–25.

[10] Freitas, C. J., Editorial - Policy Statement on the Control of Numerical Accuracy, *Journal of Fluids Engineering*, **115**, 1993, 339–340.

[11] Higuera, P., Lara, J. L. and Losada, I. J., Realistic wave generation and active wave absorption for Navier-Stokes models: Application to OpenFOAM®, *Coastal Engineering*, **71**, 2013, 102–118.

[12] Journée, J. and Massie, W., Offshore Hydromechanics, *Delft University of Technology: Delft, The Netherlands*.

[13] Larsson, L., Stern, F. and Bertram, V., Benchmarking of Computational Fluid Dynamics for Ship Flows: the Gothenburg 2000 workshop, *Journal of Ship Research*, **47**, 2003, 63–81.

[14] NASA, NPARC Alliance CFD Verification and Validation, 2018.

[15] Oberkampf, W. L. and Trucano, T. G., Verification and Validation in Computational Fluid Dynamics, *Progress in Aerospace Sciences*, **38**, 2002, 209–272.

[16] OpenCFD, L., OpenFOAM The open source CFD toolbox, 2018.

[17] Phillips, T. S. and Roy, C. J., Richardson extrapolation-based discretization uncertainty estimation for Computational Fluid Dynamics, *Journal of Fluids Engineering*, **136**, 2014, 121401.

[18] Resistance Committee of 25th ITTC, Uncertainty Analysis in CFD Verification and Validation - Methodology and Procedures, 2008.

[19] Roache, P. J., *Fundamentals of Verification and Validation*, Hermosa Publishers, 2009.

[20] Roache, P. J., Verification and validation in fluids engineering: some current issues, *Journal of Fluids Engineering*, **138**, 2016, 101205.

[21] Thiagarajan, K. and Troesch, A., Hydrodynamic heave damping estimation and scaling for tension leg platforms, *Journal of Offshore Mechanics and Arctic Engineering*, **116**, 1994, 70–76.